Uncertainty Quantification Integrated to CFD Modeling of Synthetic Jet Actuators

Srikanth Adya, Daoru Han and Serhat Hosder
Missouri University of Science and Technology, Rolla, Missouri – 65409, USA Corresponding Author; E-mail: hosders@mst.edu

[Received date; Accepted date] – to be inserted later

Abstract

The Point-Collocation Non-intrusive Polynomial Chaos (NIPC) method has been applied to a stochastic synthetic jet actuator problem used as one of the test cases in the CFDVAL2004 workshop to demonstrate the integration of computationally efficient uncertainty quantification to the high-fidelity CFD modeling of synthetic jet actuators. The test case included the simulation of an actuator generating a synthetic jet issued into quiescent air. The Point-Collocation NIPC method is used to quantify the uncertainty in the long-time averaged u and v-velocities at several locations in the flow field due to the uniformly distributed uncertainty introduced in the amplitude and frequency of the oscillation of the piezo-electric membrane. Fifth-order NIPC expansions were used to obtain the uncertainty information, which showed that the variation in the v-velocity is high in the region directly above the jet slot and the variation in the u-velocity is maximum in the region immediately adjacent to the slot. Even with a ±5% variation in the amplitude and frequency, the long-time averaged u and v-velocity profiles could not match the experimental measurements at y=0.1 mm above the slot indicating that the discrepancy may be due to other uncertainty sources in CFD and/or due to the measurement errors.

1. INTRODUCTION

Flow control involves active or passive devices that produce beneficial changes in wall bounded or free shear flows. Effective flow control can be employed to either delay or advance transition, suppress or improve turbulence or prevent or provoke flow separation depending on the application and the associated flow field. The potential benefits of realizing efficient flow control include drag reduction, lift enhancement, better mixing and noise suppression to name a few [1].

Among the flow control devices, synthetic jet actuators are one of the most-frequently studied configurations since they are highly promising in terms of realizing actual flow control system on an aircraft. In a typical synthetic jet actuator configuration, the jet is produced by a moving membrane that is built into the wall of the cavity. This jet is ejected out through an orifice that can be directly mounted on the control surface. The simplicity of the design obviates the need for complex ducting and packaging and hence a more attractive solution. Unique to synthetic jet, is also the fact that, they are formed by the working fluid in the flow system in which they are employed. This results in addition of momentum to the system without adding any mass, hence the name "zero net-mass flux jets." During the ejection half of the membrane motion, for a two-dimensional orifice, the flow separates at the sharp edges of the orifice and rolls into a pair of counter rotating vortices. These vortical structures then move away from the orifice under their own self induced velocity. In the presence of a cross-flow, these vortex pairs convect downstream entraining fluid from the free stream, resulting in favorable local displacement of the streamlines and pressure distribution changes at these regions. In recent years there have been a number of experimental and numerical investigations of the pulsating synthetic jets. A comprehensive list of these works can be found in a review paper by Glezer and Amitay [2].

The high-fidelity Computational Fluid Dynamics (CFD) simulations that can accurately predict the synthetic jet behavior are important to understand the flow physics and be able to design robust actuators that can work efficiently in various operating conditions. In order to assess the state-of-the-

art CFD modeling of these actuators, a validation workshop for synthetic jets and turbulent separation control (CFDVAL2004) [3] was held in 2004. The workshop focused on numerical formulation of a number of synthetic jet configurations, which were selected as test cases for participants. Summary of the workshop results can be found in Rumsey et al [4]. One of the conclusions of the workshop was that, due to the uncertainty involved in modeling the unsteady boundary conditions, CFD was only able to qualitatively predict the flow physics but failed to consistently achieve quantitative predictions [5]. Several parameters such as the amplitude and the angular frequency of oscillation of the diaphragm, the geometric dimensions such as the width and the height of the cavity and the slot, characterize the time dependent diaphragm deflection and the cavity flow. In real life applications, the performance of a synthetic jet actuator will be affected by the uncertainties in these parameters as well as the variation in the operating conditions such as the free stream velocity of the cross flow. In addition, the uncertainties in the physical models (i.e., turbulence models), boundary, and initial conditions used in CFD simulations will affect the accuracy of the results, which emphasizes the need for uncertainty quantification in numerical simulations.

The focus of the current study is the integration of uncertainty quantification (UQ) to the CFD modeling of synthetic jet actuators. The uncertainty quantification method will be based on nonintrusive polynomial chaos, an advanced spectral approach to propagate input uncertainty. The uncertainty information obtained for the selected output quantities of interest will be important for the assessment of the accuracy of the results and can be used in the robust and reliability based design of a synthetic jet actuator.

There have been several studies on the application of non-intrusive spectral techniques to quantify the uncertainty in CFD simulations ranging from low-order models to Large-Eddy Simulations (e.g., Lucor et. al. [6]). In a recent paper, Najm [7] gives a comprehensive review on the theory and application of polynomial chaos techniques for CFD simulations. A review on the application of non-intrusive polynomial chaos methods to fluid dynamics problems is given by Hosder and Walters [8].

An important aspect of the proposed paper will be to demonstrate the application of the Point-Collocation Non-Intrusive Polynomial Chaos (NIPC) Method to propagate the input uncertainty. In general the NIPC methods, which are based on spectral representation of the uncertainty, are computationally more efficient than the traditional Monte Carlo methods for stochastic fluid dynamic problems with moderate number of uncertain variables as shown in studies by Hosder et. al. ([8] and [9]) and can give highly accurate estimates of various uncertainty metrics. In addition, they treat the deterministic model (e.g. the CFD code) as a black box and the uncertainty information in the output is approximated with a polynomial expansion, which is constructed using a number of deterministic solutions, each corresponding to a sample point in random space. Therefore, NIPC methods become a perfect candidate for the uncertainty quantification in the high-fidelity modeling of synthetic jet actuators, since these simulations require the numerical solution of viscous, turbulent, unsteady flow fields, which can be computationally expensive and complex.

In this study, the uncertainty quantification approach is applied to the simulation of a synthetic jet actuator used as one of the test cases in the CFDVAL2004 workshop. This problem (Case 1 of CFDVAL2004) includes the modeling of a synthetic jet actuator issued into quiescent air. For this case, the oscillation frequency and the amplitude of the diaphragm velocity are treated as uncertain input variables. In the following section the numerical modeling of the synthetic jet actuator is explained. In Section 3 the Point-Collocation NIPC method is described. The uncertainty quantification results are presented in Section 4 and the conclusions are given in section 5.

2. NUMERICAL MODELING

2.1 Synthetic Jet Actuator

2.1.1 Geometry

This case uses the geometry used in Case1 of CFDVAL2004 and models a synthetic jet issuing into quiescent air out of a rectangular slot 0.05" wide and 1.4" long. The actuator is flush mounted on an aluminum plate, 0.25" thick, enclosed by a 2'×2'×2' glass enclosure. The enclosure helps to isolate the jet from the ambient air and also contains the seeding particles for the flow measurement. The slot is located at the center of the plate. Jet is produced by a circular piezo-electric diaphragm, 2" in diameter mounted on one side of the cavity beneath the plate. An O-ring seal clamps the diaphragm to the cavity, reducing the effective diameter available for oscillation, to 1.85". The diaphragm displacement is offset such that the displacement is less inwards and more outwards.

2.1.2 CFD Model

The commercial CFD software, Fluent 6.3 [10], was used for the simulations. The unsteady Reynolds-Averaged Navier-Stokes (RANS) equations coupled with two-equation eddy viscosity SST k-omega turbulence model [11] were solved to compute the unsteady, turbulent, two-dimensional flow both in the cavity and the main flow domain of quiescent air. The CFD validation workshop results indicated that a two-dimensional flow assumption gave reasonable solutions in the near-field up to a location of 8 mm measured from the slot exit. Therefore in this study we also focused on the quantification of uncertainty in the near-field flow properties with a two-dimensional approach. A pressure-based solver was used in the computations with SIMPLE algorithm for velocity-pressure coupling. The inviscid fluxes were approximated with a second-order upwind scheme in space and the viscous terms were approximated with second-order central differencing. A second–order accurate implicit time-integration scheme was used to advance the solution in time.

2.1.3 Boundary conditions

Outflow boundary condition was imposed on the left, right and top boundaries of the domain (Figure 1). The aluminum plate and the wall of the cavity were treated as no-slip wall boundaries. From the experiments, the diaphragm oscillation was available in terms of a time-dependent displacement profile measured at the center of the diaphragm [12]. For computations, a cosine curve was fit to this data and the velocity was obtained by taking the time derivative of the resulting displacement profile. Equations 1 and 2 represent the time dependent displacement and velocity of the diaphragm. In Equation 1, D represents the displacement of the center of the piezoelectric membrane, a_0 represents the amplitude of displacement (0.2863 mm) and C is a constant to account for the offset in the displacement (-0.125 mm). In Equation 2, u represents the xvelocity component of the membrane motion, A_0 is the amplitude and f is the frequency of the membrane velocity. This unsteady velocity information was then used as a time-dependent inlet velocity boundary condition in the CFD simulations. It should be noted that, the current study modeled the membrane as a piston with velocity on the entire face given by Equation 2.

$$D = a_0 cos(2\pi ft) + C \tag{1}$$

$$u = A_0 sin(2\pi ft) \tag{2}$$

2.1.4 Grid and Temporal resolution

In order to accurately reproduce the experimental and CFD results from the workshop, this study used the grid made available on the CFDVAL2004 website [12]. The grid is made up of nine zones. Two levels of grid densities were available from the workshop. The current study utilized the fine mesh with a total number of 198,545 grid points (Figure 1). As for the time step size, each cycle of the membrane oscillation was divided into 1000 time steps with each time step corresponding to 2.2487×10^{-6} seconds.

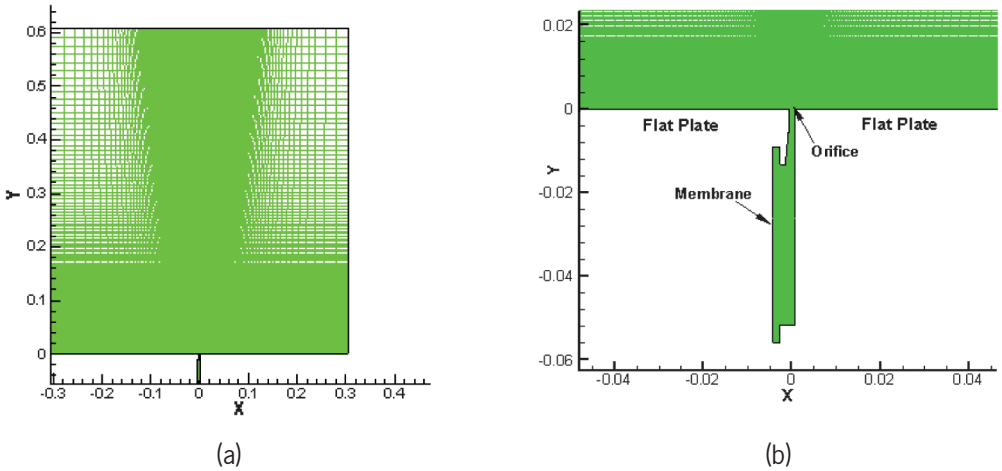

Figure 1. Computational grid for Case 1: (a) Full domain (b) Zoomed view of the cavity [8]

To achieve convergence at every time step, 15 inner iterations were performed. Figure 2 shows the u-velocity contour plot at 90 deg phase angle with the baseline configuration which gives a snapshot of the counter rotating vortex pairs, generated by the membrane oscillation, rising into the quiescent air domain. The periodicity in the output quantities was achieved after two complete cycles. The average was taken over the next cycle to obtain all the long-time averaged quantities.

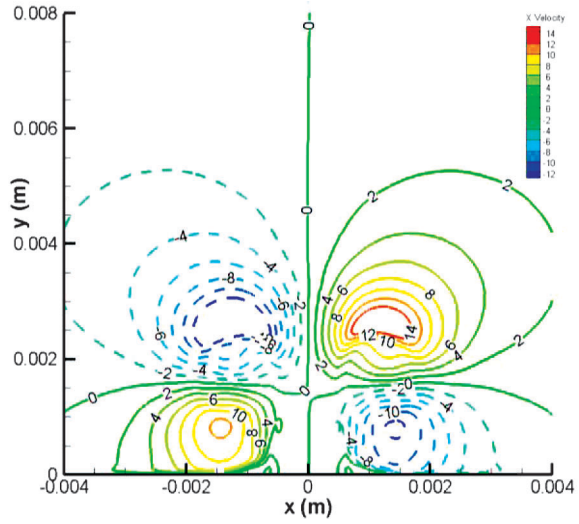

Figure 2. Instantaneous u-velocity (x-velocity) contour plot above the slot exit at 90 deg phase angle (baseline case) after the periodicity in u-velocity is achieved.

3. THE UNCERTAINTY QUANTIFICATION APPROACH

For the uncertainty quantification in the CFD simulation of synthetic jet actuators, the Point-Collocation Non-Intrusive Polynomial Chaos (NIPC) [9] Method was used to propagate the input uncertainty to the output quantities of interest. The Point Collocation NIPC is derived from polynomial chaos theory, which is based on the spectral representation of the uncertainty (see Ghanem and Spanos [13]). An important aspect of spectral representation of uncertainty is that one may decompose a random function (or variable) into separable deterministic and stochastic components. For example, for any random variable (i.e., α^*) such as velocity, density, or pressure in a stochastic fluid dynamics problem, we can write,

$$\alpha^*(\vec{x},t,\vec{\xi}) \approx \sum_{j=0}^{P} \alpha_j(\vec{x},t)\Psi_j(\vec{\xi}), \tag{3}$$

where $a_j(\vec{x}, t)$ is the deterministic component and $\Psi_j(\xi)$ is the random basis function corresponding to the jth mode. In general, α^* is a function of deterministic independent variable vector $\vec{x}$, time t, and the n-dimensional standard random variable vector $\vec{\xi} = (\xi_1, \ldots, \xi_n)$. In theory, the polynomial chaos expansion given by Equation 3 should include infinite number of terms, however in practice a discrete sum is taken over a number of output modes (or total number of terms, N_t) for a total order expansion given by

$$N_t = P + 1 = \frac{(n+p)!}{n!\,p!}, \tag{4}$$

which is a function of the order of polynomial chaos (p) and the number of random dimensions (n). The basis functions used in the stochastic expansion given in Equation 3 are polynomials that are orthogonal with respect to a weight function over the support region of the input random variable vector. The basis function takes the form of multi-dimensional Hermite Polynomial to span the n-dimensional random space when the input uncertainty is Gaussian (normal), which was first used by Wiener [14] in his original work of polynomial chaos. To extend the application of the polynomial chaos theory to the

propagation of continuous non-normal input uncertainty distributions, Xiu and Karniadakis [15] used a set of polynomials known as the Askey scheme to obtain the "Wiener-Askey Generalized Polynomial Chaos". The Legendre and Laguerre polynomials, which are among the polynomials included in the Askey scheme are optimal basis functions for bounded (uniform) and semi-bounded (exponential) input uncertainty distributions respectively in terms of the convergence of the statistics. The multivariate basis functions can be obtained from the product of univariate orthogonal polynomials (See Eldred et. al.[16]). If the probability distribution of each random variable is different, then the optimal multivariate basis functions can be again obtained by the product of univariate orthogonal polynomials employing the optimal univariate polynomial at each random dimension. This approach requires that the input uncertainties are independent standard random variables, which also allows the calculation of the multivariate weight functions by the product of univariate weight functions associated with the probability distribution at each random dimension. The detailed information on polynomial chaos expansions can be found in Walters and Huyse [17], Najm [7], and Hosder et. al [9].

To model the uncertainty propagation in computational simulations via polynomial chaos with an intrusive approach, all dependent variables and random parameters in the governing equations are replaced with their polynomial chaos expansions. Taking the inner product of the equations, (or projecting each equation onto j^{th} basis) yield $P + 1$ times the number of deterministic equations which can be solved by the same numerical methods applied to the original deterministic system. Although straightforward in theory, an intrusive formulation for complex problems (such as the high-fidelity time-dependent simulation of synthetic jet flow fields considered in this study) can be relatively difficult, expensive, and time consuming to implement. To overcome such inconveniences associated with the intrusive approach, non-intrusive polynomial chaos formulations have been considered for uncertainty propagation.The Point-Collocation NIPC starts with replacing the uncertain variables of interest with their polynomial expansions given by Equation 3. Then, P+1 (N_t) vectors ($\vec{\xi} = \{\xi_1, \xi_2, \ldots, \xi_n\}_j, j = 0, 1, 2, \ldots, P$) are chosen in random space for a given PC expansion with P +1 modes and the deterministic CFD code is evaluated at these points. With the left hand side of Equation 3 known from the solutions of deterministic evaluations at the chosen random points, a linear system of equations can be obtained:

$$\begin{bmatrix} \Psi_0(\vec{\xi}_0) & \Psi_1(\vec{\xi}_0) & \cdots & \Psi_P(\vec{\xi}_0) \\ \Psi_0(\vec{\xi}_1) & \Psi_1(\vec{\xi}_1) & \cdots & \Psi_P(\vec{\xi}_1) \\ \vdots & \vdots & \ddots & \vdots \\ \Psi_0(\vec{\xi}_P) & \Psi_1(\vec{\xi}_P) & \cdots & \Psi_P(\vec{\xi}_P) \end{bmatrix} \begin{Bmatrix} \alpha_0(\vec{x},t) \\ \alpha_1(\vec{x},t) \\ \vdots \\ \alpha_P(\vec{x},t) \end{Bmatrix} = \begin{Bmatrix} \alpha^*(\vec{x},t,\vec{\xi}_0) \\ \alpha^*(\vec{x},t,\vec{\xi}_1) \\ \vdots \\ \alpha^*(\vec{x},t,\vec{\xi}_P) \end{Bmatrix} \tag{5}$$

The spectral modes (α_k) of the random variable α^* are obtained by solving the linear system of equations given above. The solution of linear problem given by Equation 5 requires P+1 deterministic function evaluations. If more than P+1 samples are chosen, then the over-determined system of equations can be solved using a Least Squares approach. Hosder et. al. [18] investigated this option by increasing the number of collocation points in a systematic way through the introduction of an oversampling ratio n_p defined as

$$n_p = \frac{number\ of\ samples}{P+1}. \tag{6}$$

Their results on model stochastic problems showed that using a number of collocation points that is twice more than the minimum number required ($n_p = 2$) gives a better approximation to the statistics at each polynomial degree. The Point-Collocation NIPC has the advantage of flexibility on the selection of collocation points in random space (i.e., random, Latin HyperCube, Hammersley, importance sampling etc.) and possible re-use of collocation points for higher-order polynomial construction (i.e., selection of collocation points with incremental Latin Hypercube sampling). With the proper selection of collocation points, it has been shown that Point-Collocation NIPC can produce highly accurate stochastic response surfaces with computational efficiency in various stochastic fluid dynamics problems ([9], [18]).

In the current study, the uncertainty quantification is performed mainly on the long-time averaged velocity components at various locations of the synthetic jet flow field. Therefore, to construct the polynomial chaos expansions via Point-Collocation NIPC, the deterministic CFD code was evaluated

with the input corresponding to the collocation points sampled from the random space of input uncertain variable vector. For example, to construct a 5th degree polynomial chaos expansion with two uncertain input variables (Equation 4) with a oversampling ratio of 2 (Equation 6), a total number of 42 collocation points, thus 42 time-dependent CFD simulations were required. The choice of the 5th degree polynomial is based on the convergence study of the Mean, Standard Deviation, Cumulative Distribution Function (CDF), and 95% confidence intervals of the long-time averaged u and v-velocities at several locations, which has been explained in detail in section IV. Each time dependent CFD simulation was run until the periodicity in the output quantity of interest was achieved. The long-time averaged value of the output quantity was calculated from each CFD simulation. Then using these values (the RHS vector in Equation 5), the coefficients of the polynomial chaos expansion were obtained following the procedure described above. Since the approach is non-intrusive, the deterministic solver can be treated as a black-box. Hence, the outputs from Fluent were exported as data files and the coefficients of the polynomial chaos expansions were evaluated externally using a MATLAB routine that was developed, without the need to integrate this routine to the CFD solver. From the polynomial chaos expansions, various statistics such as the mean, standard deviation, the CDF, and 95% confidence interval for the output quantity of interest which can be a point quantity (pressure, velocity, vorticity, etc.) anywhere in the flow field or an integrated flow quantity (such as the lift and drag coefficients) can be calculated (See Hosder at al.[8] and [9] for details). It is also important to note that for a moderate number of input uncertainties, non-intrusive polynomial chaos methods are computationally more efficient than the traditional sampling-based methods such as Monte Carlo for uncertainty propagation.

The Point Collocation NIPC method has been previously applied to various stochastic fluid dynamics problems including low speed viscous flows, supersonic expansions and, transonic 3-D wing flow fields for uncertainty quantification (See Hosder et al, [9], [19] for details). The stochastic results of these studies have shown good agreement with Latin Hypercube Monte-Carlo results of the same cases, which were obtained for the validation of the Point-Collocation NIPC method.

4. UNCERTAINTY QUANTIFICATION RESULTS

The stochastic problem for the synthetic jet actuator was formulated by introducing uncertainties in the amplitude (A_0) and frequency (f) of the unsteady velocity inlet boundary condition used to model the oscillation of the piezo-electric membrane in the cavity (See Equation 2). The parameters $A_0 = A_0(\xi_1)$ and $f = f(\xi 2)$ were modeled as uniform uncertain variables with the mean values of 0.8 (m/s) for the amplitude and 444.7 Hz for the frequency. The uncertainty range was taken as [0.76, 0.84] (m/s) for the amplitude and [422.465, 466.935] (Hz) for the frequency, which correspond to ±5% change from the corresponding mean values to demonstrate the application of the NIPC method for uncertainty quantification. The same procedure can be followed when specific uncertainty information from experiments becomes available. Here ξ_1 and ξ_2 are standard uniform random variables defined in the interval [-1, 1], which have a constant PDF of 0.5. Due to the uniform nature of the input uncertainties, the Legendre polynomials were used as the basis functions in the polynomial chaos expansions. For the construction of the stochastic response surface with Point-Collocation NIPC, 42 number of collocation points were selected in random space by Latin Hypercube sampling (Figure 3), which corresponds to an oversampling ratio of 2 for a 5th degree polynomial of two random variables.

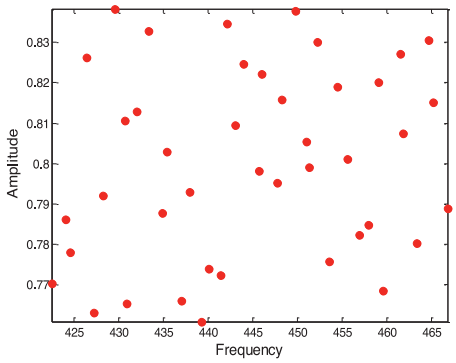

Figure 3. Collocation Points obtained with Latin Hypercube Sampling in the two-dimensional random variable space

For uncertainty quantification, long-time averaged u and v velocity components at several points along three different horizontal stations were considered (y=0.1mm, y=1mm and y=4mm above the slot exit.).

To obtain the statistics, polynomial chaos expansions at each point were evaluated with 10,000 uniform random samples $((\xi_1, \xi_2)_i$, i=1,…,10000). Note that there is no relation between the number of samples used to evaluate the statistics and the deterministic CFD simulations, which were used to obtain the coefficients of the polynomial chaos expansion given by Equation 3. Once the expansion is available one can perform a separate, large number of sampling to calculate the uncertainty statistics since evaluating the polynomial chaos expansion will be computationally inexpensive.

Figure 4 (a) through (d) shows the convergence of Mean and Standard deviation at the location x=0, y=4mm for long-time averaged u and v-velocities. It can be seen from these plots that both the mean and the standard deviation completely converge with a 5th degree polynomial. The percentage error in Mean between the 4th and the 5th degree polynomial for v-velocity at this location was found to be 0.01% and that for STD was found to be 3.42%. The percentage error in Mean between the 4th and the 5th degree polynomial for u-velocity at the same location was found to be 2.05% and that for STD was found to be 0.38%. Similar trends can be seen at all the other locations Figure 5 (a) through (d) show the CDF convergence of the long-time-averaged v and u-velocities at point (x=0,y=0.1mm) and point (x=0,y=4mm) for different polynomial orders. The convergence of the 95% confidence intervals for long-time averaged v and u velocities at y=0.1 mm and y=4 mm lines are given in Figure 6 (a) through (d). Based on these convergence studies, fifth order polynomial chaos expansions have been used to generate all the uncertainty statistics.

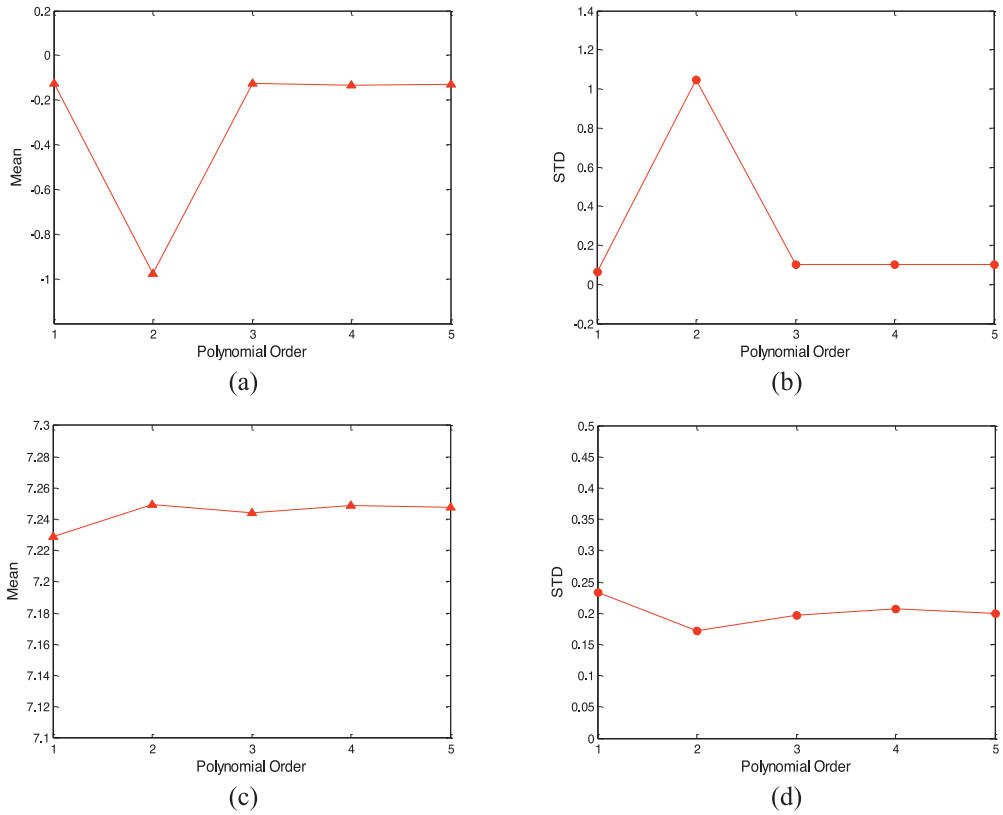

Figure 4. (a) Convergence of long-time averaged u-velocity Mean at x=0, y=4mm (b) Convergence of longtime averaged u-velocity STD at x=0, y=4mm (c) Convergence of long-time averaged v-velocity Mean at x=0, y=4mm (d) Convergence of long-time averaged v-velocity STD at x=0, y=4mm

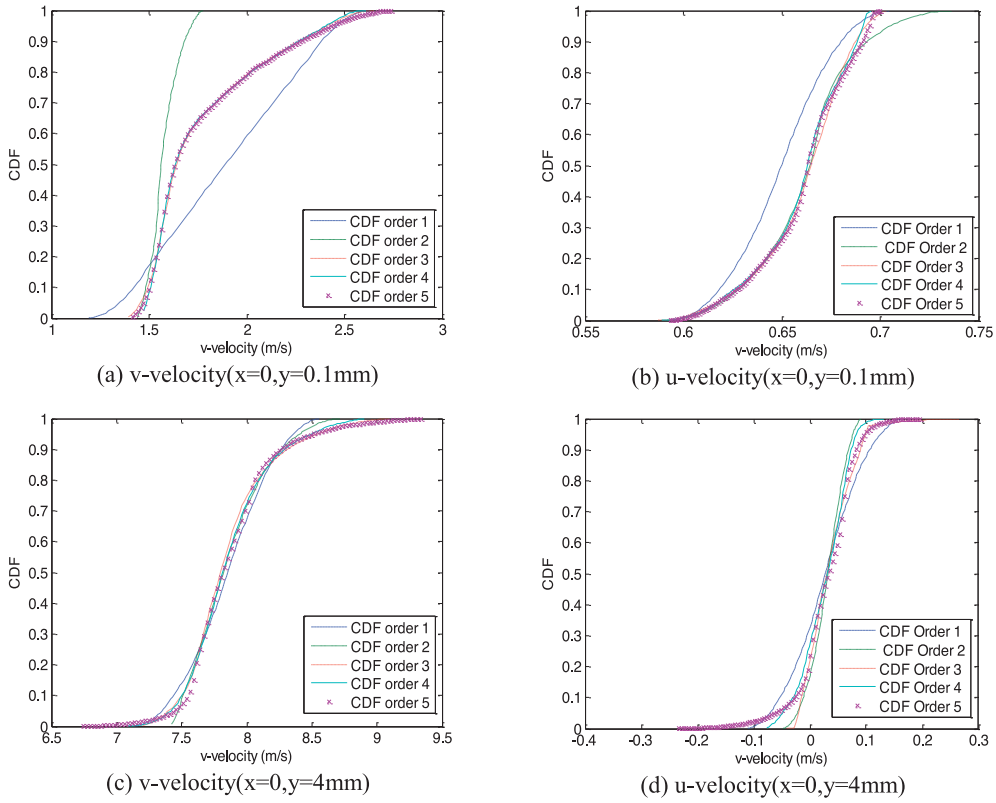

(a) v-velocity(x=0,y=0.1mm) (b) u-velocity(x=0,y=0.1mm)

(c) v-velocity(x=0,y=4mm) (d) u-velocity(x=0,y=4mm)

Figure 5. Convergence of CDFs for long-time averaged v and u-velocities at two locations

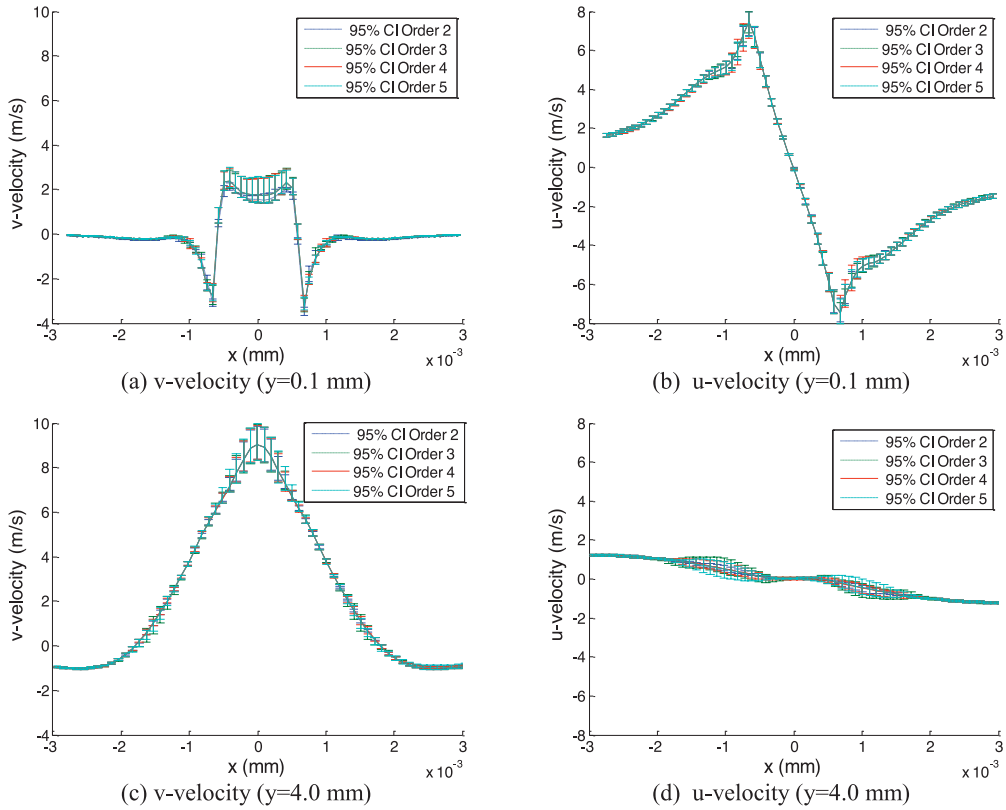

(a) v-velocity (y=0.1 mm) (b) u-velocity (y=0.1 mm)

(c) v-velocity (y=4.0 mm) (d) u-velocity (y=4.0 mm)

Figure 6. Convergence of 95% CIs for long-time averaged v and u velocities

Figure 7 shows the histograms for long-time averaged v-velocity at three different heights directly above the slot exit. It can be seen that the dependency of the v-velocity on the input stochastic variables (amplitude and the frequency of the piezo-electric membrane) is highly non-linear since the shapes of the histograms are quite different than a typical uniform distribution which was assumed for both input uncertain variables.

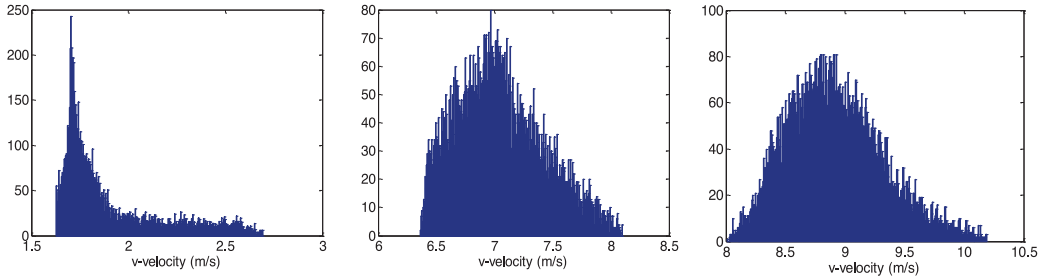

(a) x=0.0, y=0.1 mm (b) x=0.0, y=0.1 mm (c) x=0.0, y=4.0 mm

Figure 7. Histograms for long-time averaged v-velocity at three locations in the flow field.

Figure 8 shows the mean and 95% CIs for the long-time averaged u and v velocities at three constant y lines (y=0.1, 1.0, and 4.0 mm) obtained with the 5th order polynomial chaos expansions at each point. It can be seen from Figures 8 (a), (b) and (c) that the uncertainty in the v-velocity profile is higher directly above the slot exit compared to the regions to the left and right of the slot for all y stations studied. On the other hand, the uncertainty in the u velocity is minimum on the centerline (x=0.0 mm), which is consistent with the motion of the vortices above the slot. The u-velocity profiles at these locations are least uncertain due to the fact that the vortex pairs are symmetric about the centerline. The uncertainty in u-velocity is higher just adjacent to the slot on either sides as seen in Figures 8 (d), (e) and (f). It can be seen from figure 8(f) that there is a large variation induced in the region adjacent to the slot at y=4mm, above the slot exit, as a result of the uncertainty in the input amplitude and frequency. The experimental results obtained from the PIV measurements are also included in Figure 8 for reference. For the v velocity distribution at y=0.1 mm, even with a relatively large uncertainty introduced to the amplitude and the frequency of the membrane motion, the discrepancy between experiment and the simulations above the slot exit cannot be explained. The same observation can be made for the u velocity especially away from the slot exit at y=0.1 mm location. Similar trends were seen in all the other results from the CFDVal2004 workshop. This may indicate that the discrepancy at this location may be due to the other uncertainty sources in CFD (e.g., turbulence modeling or the boundary conditions) and/or the uncertainties in the measurements.

Figure 9 shows the standard deviation distribution at three different locations. As expected, the standard deviation is higher at the center of the slot for the v-velocities indicating that the variation of the long time averaged v-velocity profiles from the mean, in the region spanning the jet width, is much more compared to the regions to the left and right of the slot. Notice that the two lesser peaks on either sides of the slot width, in figure (b), are at locations where the length of the 95% CI bars momentarily increases and then gradually fades out (figure 8(b)). A similar trend can be seen in figure 9(c). Also, it can be seen from plots (d), (e) and (f) that the peaks of the standard deviation curves for the u-velocity are on either sides of the slot width and the standard deviation is minimum at the center of the slot. This is also an acceptable trend since we have seen from the 95% CI plots (figure 8 (d) to (f)) that the variation in u-velocity is more on either sides of the slot width regions and is very less at the center of the slot.

The scatter plots of the various uncertain output parameters can be easily obtained by evaluating the corresponding polynomial chaos expansions ($P(\vec{\xi})$) with a large sample of scaled input uncertain variables ($\vec{\xi}$). Figure 10 shows the scatter plot of longtime averaged v-velocity with respect to frequency and amplitude, respectively, at (x=0, y=0.1mm). With the help of these plots a Global Sensitivity Analysis can be performed using linear regression method to determine the sensitivity of the long-time averaged v-velocity (output parameter) to the variation in the input. It can be seen from figure 10(a) and (b) that the long-time averaged v-velocity at this location is highly sensitive to frequency and not as much to the amplitude. The narrow band in 10(a) indicates that for a constant frequency the

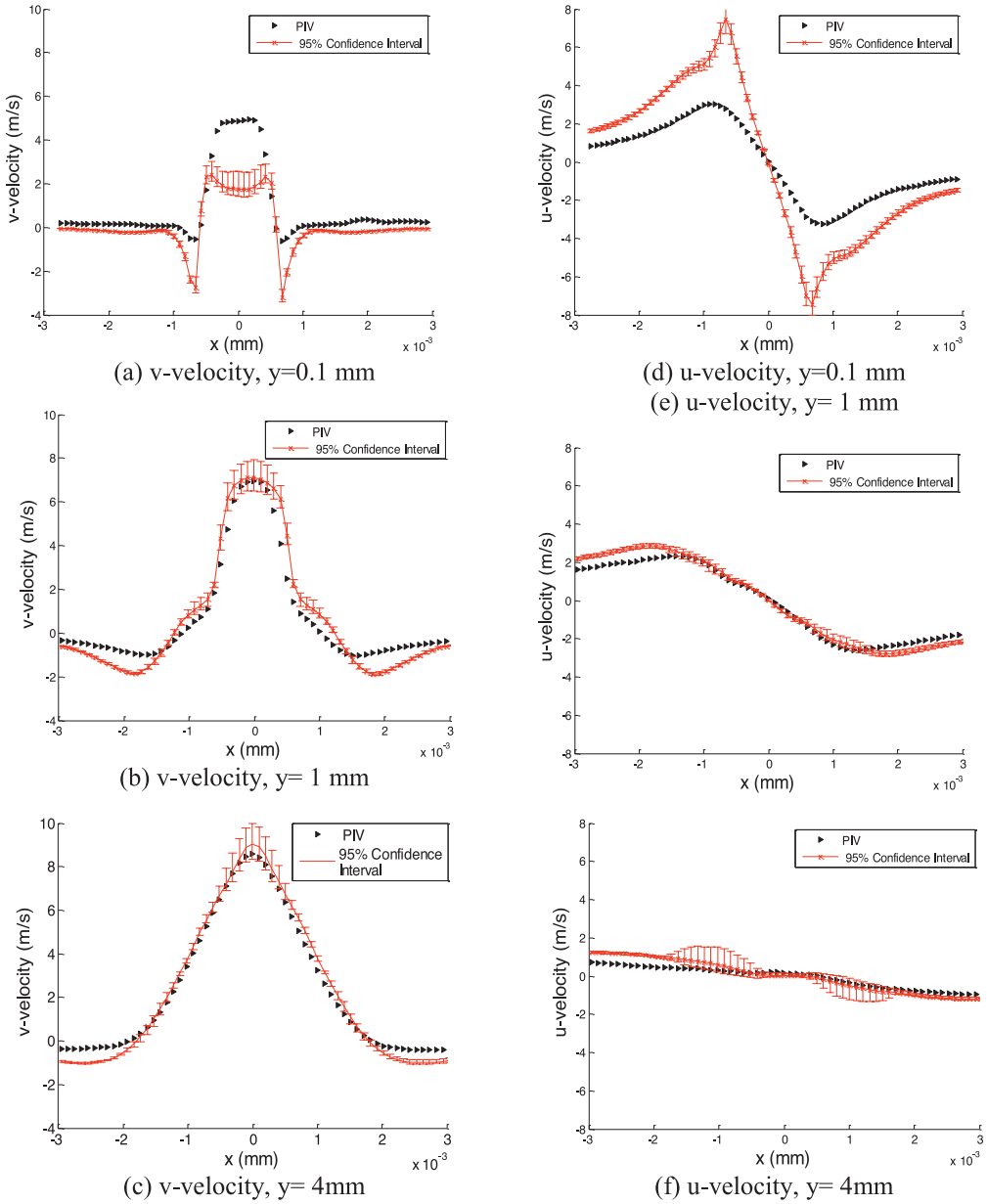

Figure 8. The mean and the 95% CIs for long-time averaged u and v-velocities at three y stations

variation in the output due to the variation in amplitude is relatively less. On the other hand, the wide scatter in 10(b) indicates that for constant amplitude, the variation in frequency causes a relatively higher variation in the output. This fact is reinforced by comparing the correlation coefficients between the output and the two input parameters. In figure 10(a) the correlation coefficient between v-velocity and frequency was found to be -0.7856 where as in 10(b) the correlation coefficient between v-velocity and amplitude was found to be 0.1319. Correlation coefficient between long-time averaged v-velocity and frequency is higher in magnitude compared to that of amplitude indicating a higher sensitivity of the output to frequency at this location.

Figure 11(a) and (b) show the scatter plots of the long-time averaged v-velocity with frequency and amplitude respectively, at x=0, y=4mm location. Here, it can be seen that both distributions are comparable. The correlation coefficient in 11(a) was found to be -0.7053 and that in 11(b) was found to be 0.7167. Hence it can be concluded that at this location both the input parameters have almost equal influence on the output.

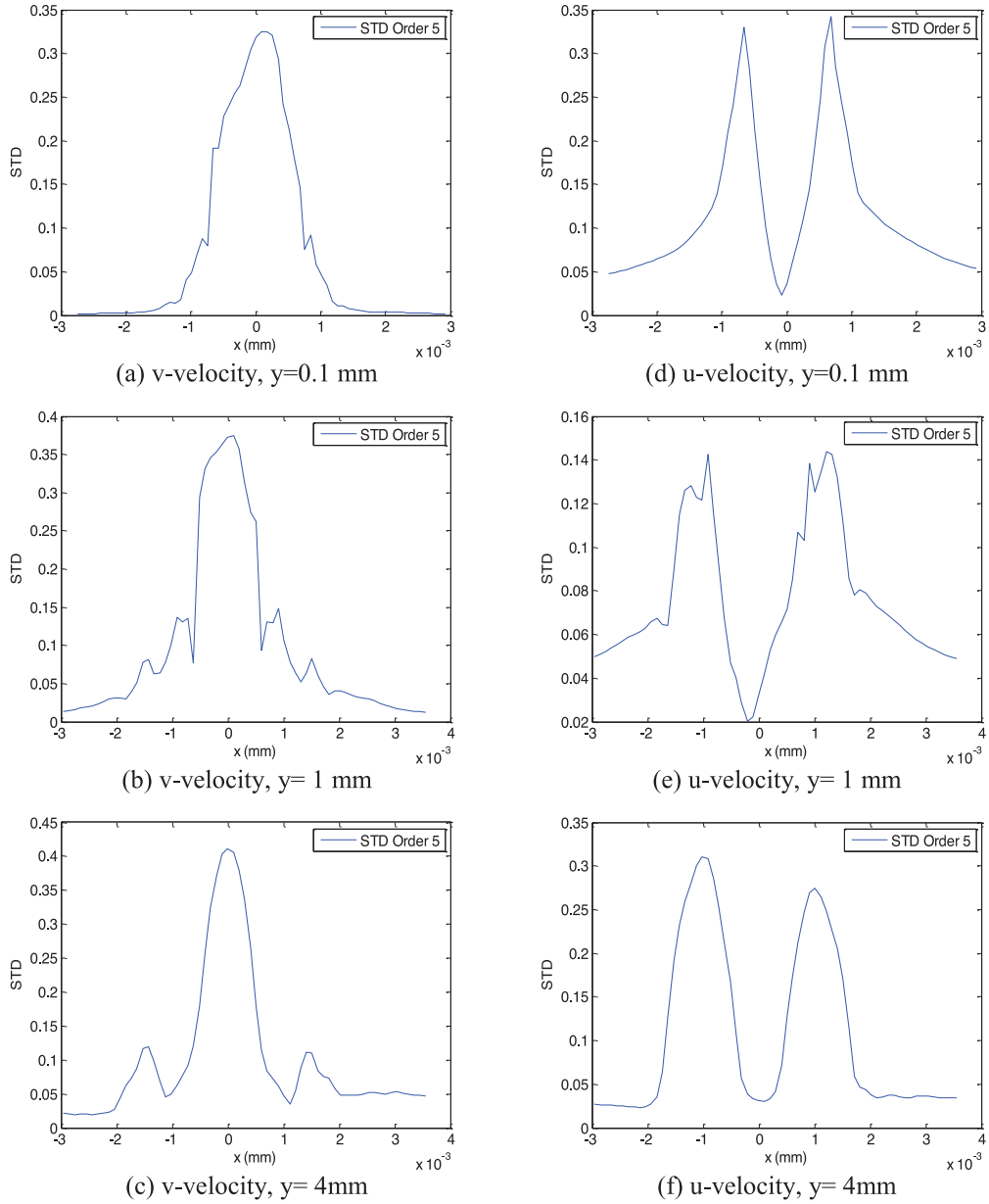

(a) v-velocity, y=0.1 mm (d) u-velocity, y=0.1 mm

(b) v-velocity, y= 1 mm (e) u-velocity, y= 1 mm

(c) v-velocity, y= 4mm (f) u-velocity, y= 4mm

Figure 9. The standard deviation (STD) distributions of long-time averaged u and v-velocities at three y stations

5. CONCLUSIONS

The Point Collocation Non-Intrusive Polynomial Chaos method has been applied to the stochastic CFD analysis of a synthetic jet problem that was used as one of the test cases in the CFDVAL2004 workshop to demonstrate the integration of computationally efficient uncertainty quantification to the high-fidelity CFD modeling of synthetic jet actuators. In the test case, a synthetic jet was issued into quiescent air and the long-time averaged u and v-velocity profiles were monitored at several locations above the slot exit. The amplitude and the frequency of the oscillation of the membrane in the cavity generating the synthetic jet were expected to have significant influence on the velocity profiles in the flow field. Therefore, the estimation of the uncertainty in long-time averaged velocity components, caused by the variation in these two parameters within the specified limits, was performed. Both uncertain variables (amplitude and frequency of oscillation of the membrane) were treated as uniform random variables. Fifth degree NIPC expansions obtained with Latin Hypercube sampling were found to be capable of estimating the statistics after a detailed convergence analysis. A total number of 42 deterministic CFD simulations were carried out with an oversampling ratio of two for creating fifth degree polynomials of two uncertain variables.

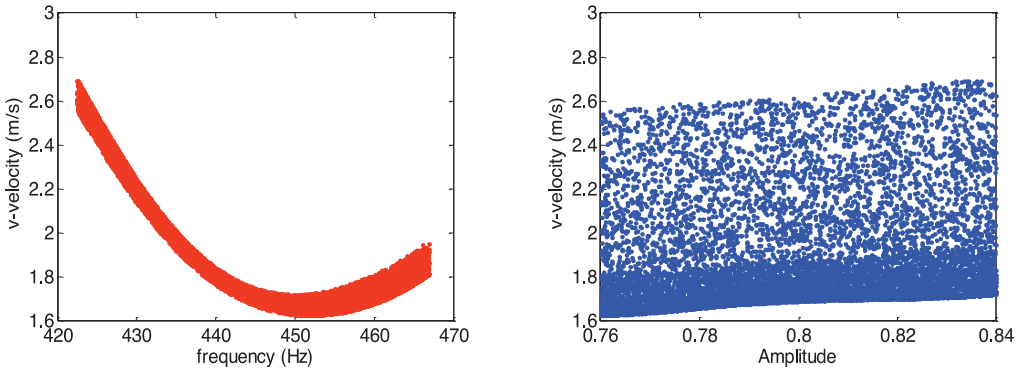

Figure 10. Scatter plots (a) long-time averaged v-velocity Vs frequency (b) long-time averaged v-velocity Vs amplitude at x=0, y=0.1mm

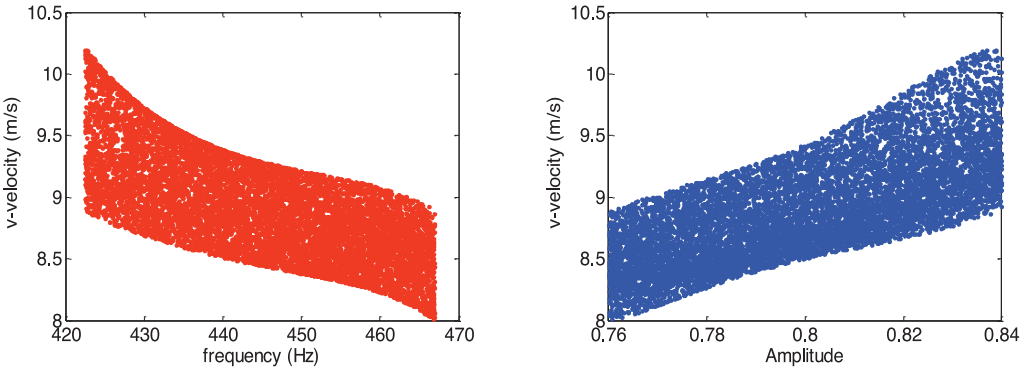

Figure 11. Scatter plots (a) long-time averaged v-velocity Vs frequency (b) long-time averaged v-velocity Vs amplitude at x=0, y=4mm

The stochastic results showed that the uncertainty in the long time averaged v-velocity was maximum at the region directly above the slot and decreased away from the center on either side. Conversely, the u-velocity variation was maximum in the region immediately adjacent to the slot and least in the region directly above the slot exit. Although both input uncertainties were modeled as uniform uncertain variables, their interaction and propagation in the flow field was found to be highly non-linear. This proves the ability of NIPC method in estimating the uncertainty statistics in non-linear problems with significantly fewer number of CFD simulations (a total number of 42) compared to those required by a typical Monte-Carlo approach. It was also found that the discrepancy between the experimentally measured values and the CFD simulations was very high at y=0.1 mm location above the slot. This could not be explained even with a relatively large uncertainty (±5% change from the mean values) introduced in the input parameters (amplitude and frequency). Hence it can be concluded that this discrepancy may be due to other uncertainty sources in CFD (e.g., turbulence modeling and boundary conditions) and/or uncertainties in the measurements.

Overall, the results obtained in this study showed the potential of Non-Intrusive Polynomial Chaos as an effective uncertainty quantification method for computationally expensive highfidelity CFD simulations applied to the stochastic modeling of synthetic jet flow fields. Our future work will include the investigation of the other uncertainty sources, especially the turbulence modeling parameters, for the same test case studied in this paper. In addition, the future work will include the consideration of sythetic jet cases with cross-flow, which will focus on the uncertainty sources associated with both the main flow and the cavity region actuating the sythetic jet. It is hoped that the uncertainty quantification results obtained for various sythetic jet cases will help the researchers to understand the effect of

different uncertainty sources on the performance of the sythetic jet actuators, which can be used for the design of robust actuator configurations.

ACKNOWLEDGEMENTS

The authors would like to acknowledge University of Missouri Research Board for providing support for this work.

REFERENCES

[1] Mohamed Gad-el-Hak, "Flow Control , Passive Active and Reactive Flow Management."

[2] Glezer, A., and Amitay, M., "Synthetic Jets," *Annual Review of Fluid Mechanics*, Vol. 34, 2002, pp. 503–529.

[3] "Proceedings of the 2004 Workshop on CFD Validation of Synthetic Jets and Turbulent Separation Control", compiled by Christopher L. Rumsey.

[4] Rumsey, C. L., Gatski, T. B., Sellers, W. L., III, Vatsa, V. N., and Viken, S. A., "Summary of the 2004, Computational Fluid Dynamics Validation Workshop on Synthetic Jets," *AIAA Journal*, Vol. 44, No. 2, 2006, pp. 194–207.

[5] Rumsey, C. L., "Successes and Challenges for Flow Control Simulations," *International Journal of Flow Control*, Vol. 1, No. 1, March 2009, pp. 1-27. (Survey of CFDVAL2004 case results that were published after the workshop)

[6] D. Lucor, J. Meyers & P. Saugat, "Sensitivity Analysis of Large-Eddy Simulations to Subgrid-Scale-Model Parametric Uncertainty", *J. Fluid Mechanics* (2007), Vol. 585, pp. 255-279

[7] Najm, H. N., "Uncertainty Quantification and Polynomial Chaos Techniques in Computational Fluid Dynamics," *Annual Review of Fluid Mechanics*, Vol. 41, 2009, pp. 35–52.

[8] Hosder, S. and Walters, R. W., "Non-Intrusive Polynomial Chaos Methods for Uncertainty Quantification in Fluid Dynamics, AIAA-Paper 2010-0129," *48th AIAA Aerospace Sciences Meeting*, Orlando, FL, January 4-7, 2010.

[9] Hosder, S., Walters, R. W., and Balch, M., "Point-Collocation Nonintrusive Polynomial Chaos Method for Stochastic Computational Fluid Dynamics," *AIAA Journal*, Volume 48, Number 12, December 2010.

[10] FLUENT Technical Manual.

[11] Menter, F. R., "Two-Equation Eddy-Viscosity Turbulence Models for Engineering Applications," *AIAA Journal*, Vol. 32, No. 8, 1994, pp.1598–1605

[12] Langley Research Center Workshop CFD Validation of Synthetic Jets and Turbulent separation Control website http://cfdval2004.larc.nasa.gov/.

[13] Ghanem, R. G. and Spanos, P. D., *Stochastic Finite Elements: A Spectral Approach*, Springer-Verlag, New York, 1991.

[14] Wiener, N., The Homogeneous Chaos, *American Journal of Mathematics*, Vol. 60, No. 4, 1938, pp. 897–936.

[15] Xiu, D. and Karniadakis, G. E., "Modeling Uncertainty in Flow Simulations via Generalized Polynomial Chaos," *Journal of Computational Physics*, Vol. 187, No. 1, May, 2003, pp. 137–167.

[16] Eldred, M. S., Webster, C. G., and Constantine, P. G., "Evaluation of Non-Intrusive Approaches for Wiener-Askey Generalized Polynomial Chaos, AIAA-Paper 2008-1892," *10th AIAA Non-Deterministic Approaches Forum*, Schaumburg, IL, April, 2008.

[17] Walters, R. W. and Huyse, L., "Uncertainty Analysis for Fluid Mechanics with Applications," Tech. rep., ICASE 2002-1, NASA/CR-2002-211449, NASA Langley Research Center, Hampton, VA, 2002.

[18] Hosder, S., Walters, R. W., and Balch, M., "Efficient Sampling for Non-Intrusive Polynomial Chaos Applications with Multiple Input Uncertain Variables, AIAA-Paper 2007-1939," *9th AIAA Non-Deterministic Approaches Conference*, Honolulu, HI, April, 2007.

[19] Hosder, S., Maddalena, L., "Non-Intrusive Polynomial Chaos for the Stochastic CFD Study of a Supersonic Pressure Probe", AIAA-Paper 2009-1129.